Gravitational Radiation from Encounters with Compact Binaries in Globular Clusters

Marianna Mao

under the direction of
Professor Edmund Bertschinger
Sarah Vigeland
Phillip Zukin
Massachusetts Institute of Technology

Research Science Institute
July 29, 2008

Abstract

When the Laser Interferometry Space Antenna is launched, compact binaries in globular clusters will be particularly interesting objects of study. The purpose of this project was to model the orbits of compact binaries in globular clusters when they are perturbed by third body stars. The models were used to calculate the trajectories, gravitational wave luminosity as a function of time, and the strain tensor $\bar{h}_{ij}$ as a function of time. Three situations were analyzed: when the binary is perturbed but remains stable, when the binary is completely scattered, and when one of the original bodies in the binary is ejected while the other two bodies enter a stable orbit.

1 Introduction

In Einstein's general theory of relativity, the spacetime continuum is a manifold combining the three dimensions of space with time as the fourth dimension. According to general relativity, a given stress-energy tensor, which describes the density and flux of energy in spacetime, determines the metric tensor of spacetime via the Einstein field equations. Thus, a distribution of various forms of energy—mass, momentum, pressure, and stress—causes the geometry of spacetime to be curved and non-Euclidean. The Newtonian concept of gravity describes a linearly directed force between bodies with mass. In general relativity, gravity is not treated as a true force but as a consequence of the geometry of spacetime: energy curves spacetime, which affects the geodesic and thus the motion of some body. General relativity predicts that light is affected by gravity in the same way that matter is, a phenomenon which has been verified by gravitational lensing.

A gravitational wave is a radiating change in spacetime curvature which propagates when the second time derivative of the quadrupole moment of a system's stress-energy tensor is non-zero. The strongest evidence to date for the existence of gravitational waves comes from Joseph Taylor's observations of binary pulsar PSR B1913+16 from 1974 to 1982. Stars in such an orbit should lose energy through the emission of gravitational waves, inspiralling and drawing closer to each other. By timing radio emissions from the pulsar, Taylor concluded that the binary was inspiralling at within 0.2 percent of the rate predicted by general relativity [1].

Gravitational waves are important because they may enable observations of black holes, binaries with compact components, the universe right after the Big Bang, and quantum fields in the early universe, all of which are impossible to detect with any form of electromagnetic radiation [2]. Their existence will also confirm parts of the theory of general relativity.

The ground-based Laser Interferometer Gravitational-Wave Observatory (LIGO) was es-

tablished to directly confirm the existence of gravitational waves and started operating in 2002. The Laser Interferometer Space Antenna (LISA) is a planned space-based observatory for gravitational waves sensitive to a lower frequency band (0.1 to 0.0001 Hz) than LIGO. Specifically, it will detect gravitational waves generated by the coalescence of massive black holes at the centers of merging galaxies, radiation from ultra-compact binaries, and the in-fall of small black holes, neutron stars, and white dwarfs into massive black holes at galactic centers [3]. Its launch is currently planned for 2015.

Compact binaries with short periods (less than one hour) in globular clusters, which are spherical formations of stars around a galactic core, are also projected observational targets for LISA. Compact binaries are systems in which two compact objects, such as white dwarfs or neutron stars, orbit a common center. Though less than 50 accreting compact binaries are known today, LISA will likely make it possible to detect several thousand new compact binaries. The LISA measurements will provide information about the phases of binary formation and evolution that is very different from what can be deduced from observations of electromagnetic radiation. The population of compact binaries in globular clusters is conjectured to be high relative to the number found in the rest of the universe. Thus, LISA will probe the rate of production of accreting compact binaries with white dwarf components in globular clusters by determining the number of such binaries [3].

To take advantage of LISA's observational abilities, predictions of the gravitational wave signatures of specific events of interest are useful. This paper analyzes the trajectories, strain tensor as seen along various axes, and the gravitational wave luminosity as a function of time when a compact binary with white dwarf components in a globular cluster is perturbed by a third star.

2 Background

2.1 Equations

Einstein summation convention is used here; it is covered in Appendix A. The formulas presented in this paper are in geometrized units with $G = c = 1$.

Einstein's field equation

$$G_{\alpha\beta} = 8\pi T_{\alpha\beta} \tag{1}$$

expresses the Einstein tensor $G_{\alpha\beta}$, which describes the curvature of spacetime, as a function of the stress-energy tensor $T_{\alpha\beta}$. Assuming that waves produced by the source $T_{\alpha\beta}$ are weak, the corresponding space-time metric $g_{\alpha\beta}$ can be written as a perturbation of the metric of flat spacetime, $\eta_{\alpha\beta}$ = diag(-1,1,1,1):

$$g_{\alpha\beta}(x) = \eta_{\alpha\beta} + h_{\alpha\beta}(x) \tag{2}$$

where $h_{\alpha\beta}$ is the strain tensor with $|h_{\alpha\beta}| \ll 1$ for all α, β. $\eta_{\alpha\beta}$ is known as the Minkowski metric.

It is useful to define the trace-reversed perturbation $\bar{h}_{\alpha\beta}$:

$$\bar{h}_{\alpha\beta} \equiv h_{\alpha\beta} - \frac{1}{2}\eta_{\alpha\beta}h \tag{3}$$

where h is simply the trace. Gravitational waves are linearly polarized in two directions: h^+ and $h^\times$. In order to calculate the radiation propagating in direction x^i, the transverse traceless gauge of $\bar{h}_{ij}$ is taken by making all x^i components in $\bar{h}_{ij}$ zero and subtracting out the trace.

Assuming that the source $T_{\alpha\beta}$ is moving at non-relativistic speeds, if the characteristic dimension of the source is much smaller than the wavelength of the propagating wave, and

that observations are made a large distance r away from the source, the strain tensor becomes

$$\bar{h}^{ij}(t,\vec{x}) = \frac{2}{r}\ddot{I}^{ij}(t-r) \tag{4}$$

where $I^{ij}(t)$ is defined as the second mass moment:

$$I^{ij}(t) \equiv \int \mathrm{d}^3x\mu(t,\vec{x})x^i x^j \tag{5}$$

where $1 \leq i,j \leq 3$. We now define the mass quadrupole moment $\not{I}^{ij}$:

$$\not{I}^{ij} \equiv I^{ij} - \frac{1}{3}\delta^{ij}I \tag{6}$$

where $\delta^{ij} = 1$ is the Kronecker delta, and where I is the trace of the second mass moment.

The formula for luminosity, or total power loss through gravitational radiation,is

$$L_{GW} = \frac{1}{5}\langle \dddot{\not{I}}_{ij} \dddot{\not{I}}^{ij} \rangle \tag{7}$$

where the brackets indicate time average. By definition we have

$$I_{ij} = g_{i\alpha}g_{j\beta}I^{\alpha\beta} \tag{8}$$

$$= (\eta_{i\alpha} + h_{i\alpha})(\eta_{j\beta} + h_{j\beta})I^{\alpha\beta} \tag{9}$$

But since we are assuming that $|h_{\alpha\beta}| \ll 1$, we may neglect all first-order terms and above that contain h. Therefore,

$$I_{ij} \approx \eta_{i\alpha}\eta_{j\beta}I^{\alpha\beta} \tag{10}$$

and

$$L_{GW} = \frac{1}{5}\sum_{i=1}^{3}\sum_{j=1}^{3} \dddot{\not{I}}_{ij} \dddot{\not{I}}^{ij} \tag{11}$$

We now have all the necessary equations to proceed with numerical analysis of the strain tensor and luminosity, given a binary-single star system.

2.2 A Circular Binary

Expressions for the strain tensor and luminosity are analytically derived for a binary system with components of equal mass M in circular orbits with orbital frequency $\omega = \frac{2\pi}{T}$ where T is the period.

We place the two bodies on the xy-plane. We let the trajectory of the first mass be $(Rcos(\omega t), Rsin(\omega t), 0)$. The other mass then has trajectory $(-Rcos(\omega t), -Rsin(\omega t), 0)$. From Equation 5, we get for the binary system

$$I^{11} = MR^2[1 + cos(2\omega t)]$$

$$I^{12} = I^{21} = MR^2 sin(2\omega t)$$

$$I^{22} = MR^2[1 - cos(2\omega t)]$$

$$I^{13} = I^{31} = I^{23} = I^{32} = I^{33} = 0$$

Now from Equation 4,

$$\bar{h}^{ij} = -\frac{8\omega^2 MR^2}{r} \begin{pmatrix} cos[2\omega(t-r)] & sin[2\omega(t-r)] & 0 \\ sin[2\omega(t-r)] & -cos[2\omega(t-r)] & 0 \\ 0 & 0 & 0 \end{pmatrix}. \tag{12}$$

We can see from the strain tensor that the frequency of the emitted radiation is twice the orbital frequency. This result is expected because of the symmetry: when the two components have equal masses in a circular orbit, the fundamental period of the binary

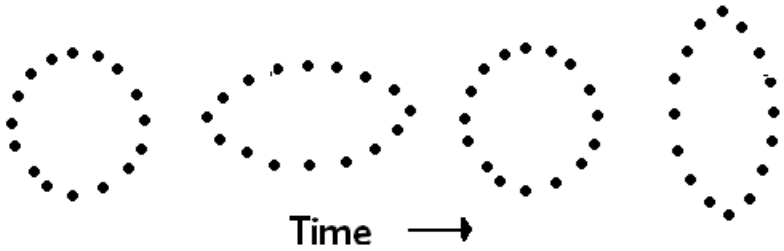

Figure 1: The effect of the h^+ polarization.

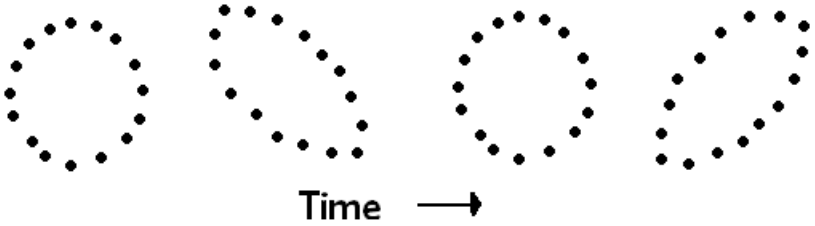

Figure 2: The effect of the $h^\times$ polarization.

becomes $\frac{T}{2}$. This representation of $\bar{h}^{ij}$ is already in transverse traceless gauge for propagation in the z direction. We get that the h^+ polarization varies as $cos[2\omega(t-r)]$ and the $h^\times$ polarization varies as $sin[2\omega(t-r)]$. Physically, the h^+ polarization indicates a wave which affects spacetime such that if propagating along the axis of a ring of test particles, the particles would be affected as in Figure 1. The $h^\times$ polarization would affect the same ring as in Figure 2.

Next, from Equation 7, we get that the luminosity, or power loss, is constant:

$$L_{GW} = \frac{128}{5} M^2 R^4 \omega^6 \tag{13}$$

This is only if we assume that power loss through gravitational radiation is negligible, which, over short periods of time, is true. This result seems reasonable because of the symmetry of

circular binaries; there is no reason why the luminosity would vary with time.

Unfortunately, analytical calculations are impossible for more complex situations, which is why we turn to numerical calculations and models.

3 Methods

3.1 Initial Parameters and Assumptions

First, gravitational effects are the dominating forces in compact binary star systems. Also, the effects due to the finite sizes of the bodies are small. Furthermore, at the low frequencies in the LISA band, the gravitational wave spectrum is dominated by detached and semidetached double white dwarfs [5]. Therefore, mass exchange and tidal interactions may be neglected. Secondly, because gravitational radiation tends to circularize binary orbits rapidly, the orbits of most such compact binaries can be treated as circular [5]. Thus, a model of a compact binary as having a circular orbit with point mass components is sufficient.

The typical globular cluster is about 10 kpc away from Earth, so r is taken to be 10^{20} meters [5]. However, LISA will be capable of resolving individual binaries up to 100 kpc away. The period of the compact binaries relevant to the problem is taken to be about 2000 seconds, producing gravitational radiation at 0.001 Hz which falls within LISA's frequency band of 10^{-1} to 10^{-4} Hz. Stars in globular clusters have a typical velocity of 10^4 meters per second and average separation in the middle region of globular clusters is on the order of 10^{15} meters, though separation can be on the order of 10^{14} in the dense core and beyond 10^{16} when sufficiently far from the core [5]. Because trajectories of the three bodies were modelled with initial separation between the binary and the third body on the order of 10^{11} meters, the energy gain due to decrease in gravitational potential was taken into account when calculating initial parameters.

3.2 Numerical Analysis

To model the trajectories of 3 bodies interacting in 3 dimensions under the force of gravity alone, a fourth-order Runge-Kutta integrator was used to solve a system of 18 differential equations given initial parameters of positions, velocities, and masses. A relative tolerance of 10^{-5} was used for the integrator. The code can be found in appendix B.

To calculate the strain tensor and luminosity, the second and third time derivatives of the second mass moment were computed by fitting cubic splines to each element of the tensor.

4 Results

Three cases are considered. In case 1, the binary is perturbed by a third body. In case 2, an exchange interaction between the binary and third body takes place. In case 3, the third body completely scatters the binary.

In the trajectory plots, a blue trajectory denotes body 1, a green trajectory denotes body 2, and a red trajectory denotes body 3. Body 3 is always the third body, and bodies 1 and 2 are the components of the compact binary.

Given the period T of a binary and masses m_1 and m_2 of the two components, a program was used to calculate the diameter of the circular orbit ($2R$) and the velocities of both bodies ($\pm v$). Bodies 1 and 2 were always set to initial positions of $(R, 0, 0)$ and $(-R, 0, 0)$ respectively, with initial velocities $(0, v, 0)$ and $(0, -v, 0)$ respectively.

The initial parameters can be found in Table 1. Mass is expressed in solar masses, distance in meters, and time in seconds. m_3 is the mass of the third body, $\vec{x}_3$ is its initial position and $\vec{v}_3$ is its initial velocity.

Case	m_1	m_2	m_3	T	$\vec{x}_3$	$\vec{v}_3$
1	1.4	1.4	1	1500	$(0, 1000R, 0, 0)$	$(0, 0, -5 \cdot 10^5)$
2	1	1	1	1500	$(0, 0, 200R)$	$(0, 10^4, -6 \cdot 10^4)$
3	.6	.6	.8	2000	$(400R, 0, 0)$	$(-2 \cdot 10^6, 100, 0)$

Table 1: Initial parameters for the three cases.

4.1 Case 1

In case one, the third star interacts with the binary and exits the system. The binary is perturbed but the components remain in a stable, although more eccentric, orbit.

In this example, the third body approaches at an angle from above the binary (Figure 3). As body 3 and the binary converge, body 3 enters a brief stable orbit with body 2 (Figure 4), ejecting the more massive body 1 from the binary. However, body 3 quickly falls out of the binary, and eventually the original binary reemerges with an eccentric orbit.

Before the 3-body interaction takes place, the luminosity is almost constant because it is dominated by the power generated from the binary (Figure 5). Small oscillations are present in the luminosity because as body 3 approaches, the binary gains linear momentum and due to the asymmetry of body 3's velocity, becomes slightly perturbed. The fairly periodic luminosity from $1.43 \cdot 10^5$ seconds to $1.47 \cdot 10^5$ seconds reflects the brief stable orbit between bodies 2 and 3. Eventually, as the binary emerges in an eccentric orbit, the luminosity once again becomes periodic.

Similar patterns are observed in the strain tensor plots as a function of time. In both the x and z directions, the strain before the 3-body interaction is dominated by the binary's gravitational radiation (Figures 6 and 7). The strain in direction y has not been depicted because the initial conditions are almost symmetric for x and y. Periodic strain variations from $1.43 \cdot 10^5$ seconds to $1.47 \cdot 10^5$ are also apparent, due to the orbit between body 3 and body 2. Periodic strain amplitudes are reestablished after the original binary and body 3 diverge.

Another type of interaction which can perturb a binary is when a third body passes by closely, but not close enough to interact with the individual components of the binary (Figure 8). In this case, a "slingshot" effect is often seen in which body 3 initially has enough momentum to shoot just past the binary; as the distance between the binary and third body decreases, the gravitational force is strong enough to cause the bodies to shoot back towards each other. It was observed that in such cases, often the binary would emerge only slightly perturbed. The resulting gravitational signal was not very informative, so it has not been included. However, because this type of interaction occurs with a very wide range of parameters, it should be the most common binary-star interaction to occur.

4.2 Case 2

A second possibility is for the third body to interact with the binary in such a way that one of the binary components is ejected, and the third body enters a stable orbit with the other star in the binary. In the example below, this scenario actually occurs twice—a rare event.

Approaching from above, body 3 undergoes complicated interactions with the binary (Figure 9). Initially, body 2 is ejected from the binary while bodies 1 and 3 enter a stable orbit (Figure 10). The new binary and body 2 meet once again and interact. The second time, body 1 is ejected and bodies 2 and 3 enter a stable orbit (Figure 11). During this interaction, bodies 1 and 2 re-enter a binary orbit for some time before body 1 is ejected.

The plot of luminosity versus time reveals exchange events at the times where either of the bodies are ejected (Figure 12). As expected, the initial and final luminosities are dominated by the constant gravitational radiation from the stable initial and final binaries.

A general idea of the strain tensor in the z and x directions can be seen in Figures 13 and 16. Before the first exchange interaction, the strain tensor plot is dominated by the binary gravitational radiation (Figures 14 and 15). After the first exchange, the strain tensor forms a far more erratic pattern. During the second exchange event, when bodies 1

and 2 reestablish a stable orbit from $2.01 \cdot 10^6$ to $2.11 \cdot 10^6$ seconds, the strain amplitudes oscillate periodically in a pattern resembling that of binary radiation (Figures 15 and 18). As the exchange event ends and a new stable orbit is formed, the strain tensor plot remains oscillating and periodic, but in a different pattern corresponding to the properties of the final binary.

4.3 Case 3

The third possibility is that the third star completely scatters the binary, not entering a stable orbit with either of the components.

In this example, body 3 approaches the stable binary at a high velocity, completely scattering bodies 1 and 2 (Figure 19). Body 2 escapes from the binary because of the strong gravitational force from body 3 as it approaches. After body 2 escapes, body 1 shoots off linearly (Figure 20).

The luminosity as a function of time is initially dominated by the constant gravitational radiation from the binary, as expected (Figure 21). The luminosity peaks as the third body interacts extremely quickly with the binary, scattering it. The luminosity then drops to a lower value than before, as expected, because the stars slow down as they move away from each other after the scattering event.

The scattering events and resulting energy loss are also evident in the strain tensor versus time plots (Figures 22 and 23). In the z-direction, the strain tensor oscillates sinusoidally due to the dominating binary interaction. The h^+ component is an almost constant value higher than the $h^\times$ component due to the motion of body 3. In the x direction, the $h^\times$ component has amplitude 0 as expected, while the h^+ component oscillates. After the binary is scattered, the oscillating pattern characteristic of binaries is gone: the amplitudes flatten out, as expected for three bodies in approximately linear motion.

5 Conclusion

Under the assumptions of long wavelengths, weak space-time curvature, and large separation from radiation sources, approximations of the Einstein field equations with linearized gravity were used to calculate the strain tensor and gravitational wave luminosity as a function of time from single star encounters with compact binaries in globular clusters. The binaries were modelled as point masses with circular orbits. Because of time constraints, parameters were chosen carefully to see what interesting 3-body interactions would result. However, because the properties of the stars and encounters are inherently stochastic, it would be desirable to use Monte Carlo simulations to test for a broad range of situations and initial parameters.

To calculate the frequency of such encounters, work done by Steinn Sigurdsson and E.S. Phinney could be extended. In 1994, they ran simulations of globular clusters with a wide range of initial parameters to tabulate the number of binary-single star exchange interactions over a period of time [6].

At a gravitational wave frequency of about 0.001 Hz, LISA's strain sensitivity is about 10^{-22}. The amplitude of the strain for the various cases has been shown to vary anywhere from on the order of 10^{-23} to 10^{-21}, depending on which polarization is being detected and on the orientation of the detector relative to the system. The strain amplitude will also be dependent on the masses of the interacting bodies, as well as how far away the source is; although r was taken to be 10^{20} meters, LISA will be able to resolve binaries in globular clusters up to 10^{21} meters away, a range which encompasses globular clusters in galaxies beyond the Milky Way.

6 Acknowledgments

I would like to thank Allison Gilmore for her support as my tutor; Phillip Zukin, Sarah Vigeland and Professor Edmund Bertschinger for their help with this project and paper; Daniel Vitek, John Shen, Austin Webb, and Andrew Shum for their helpful comments; and finally, RSI and CEE for the opportunity to research here this summer.

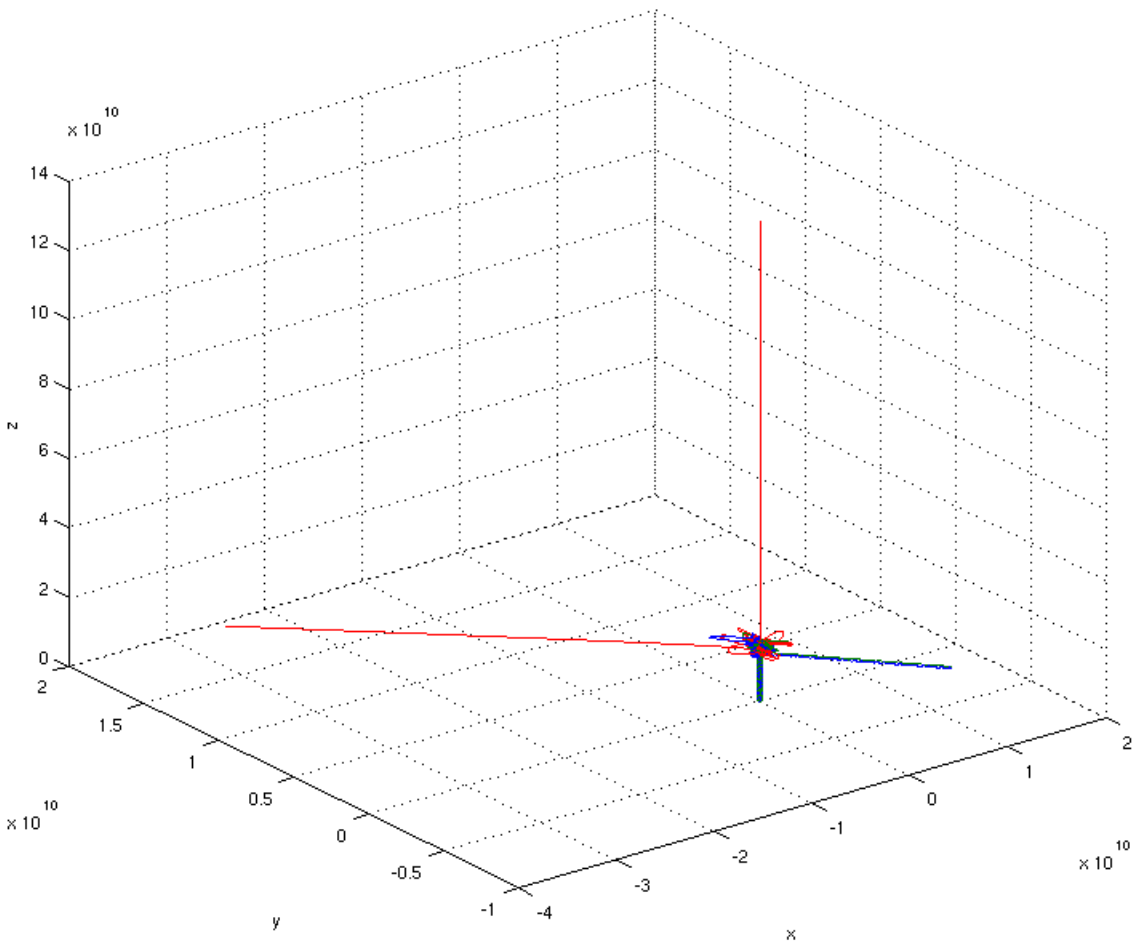

Figure 3: The trajectory for an interaction between a third body and a binary which leaves the binary perturbed.

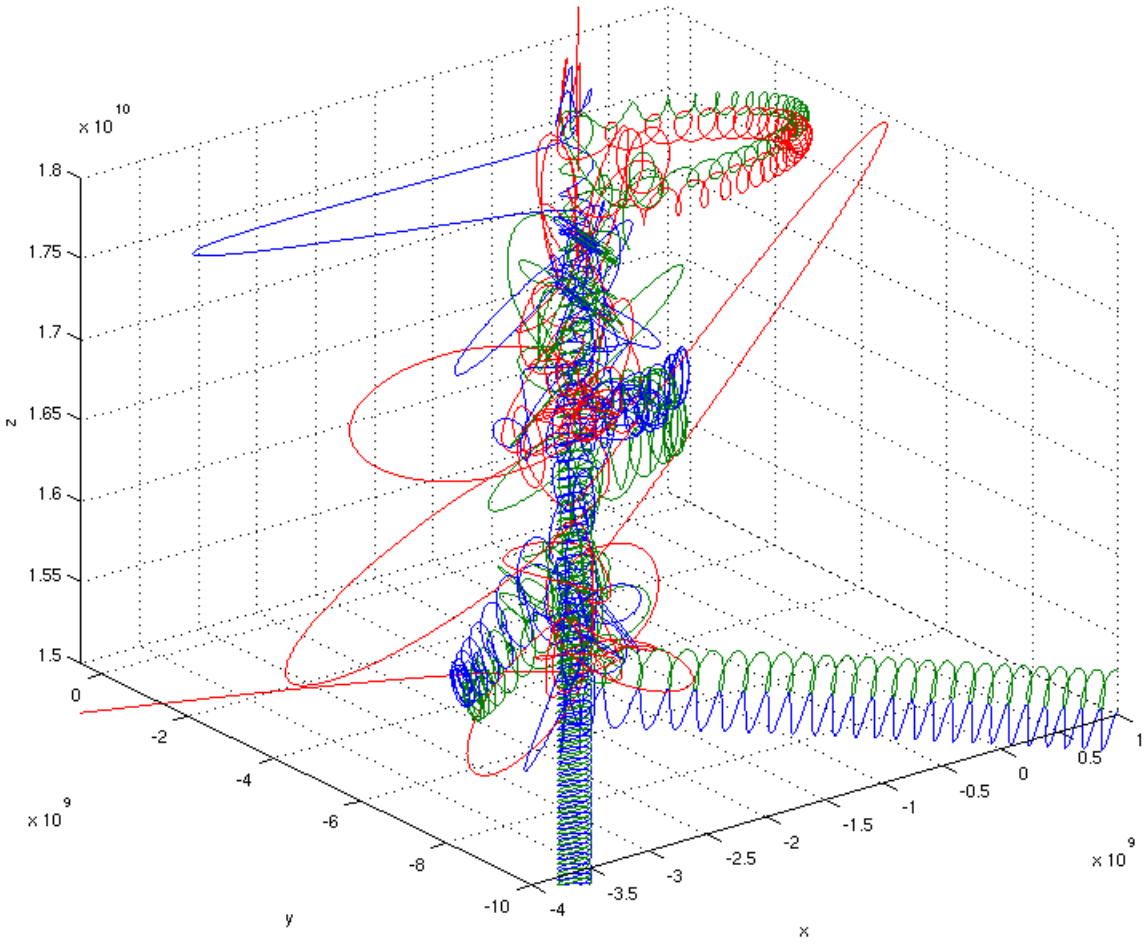

Figure 4: Close-up on the trajectory in figure 3. The binary eventually emerges in an eccentric orbit.

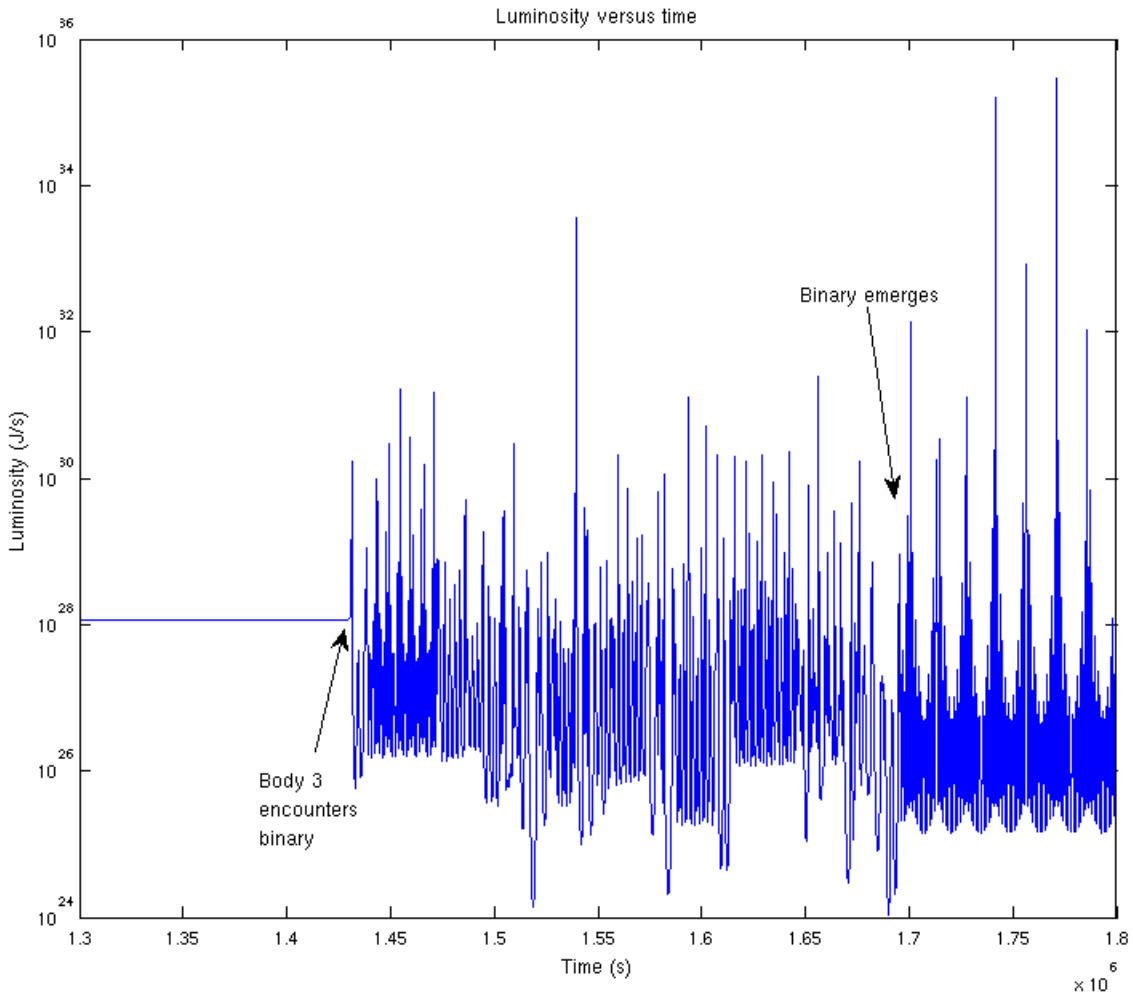

Figure 5: Luminosity versus time is shown on a logarithmic scale.

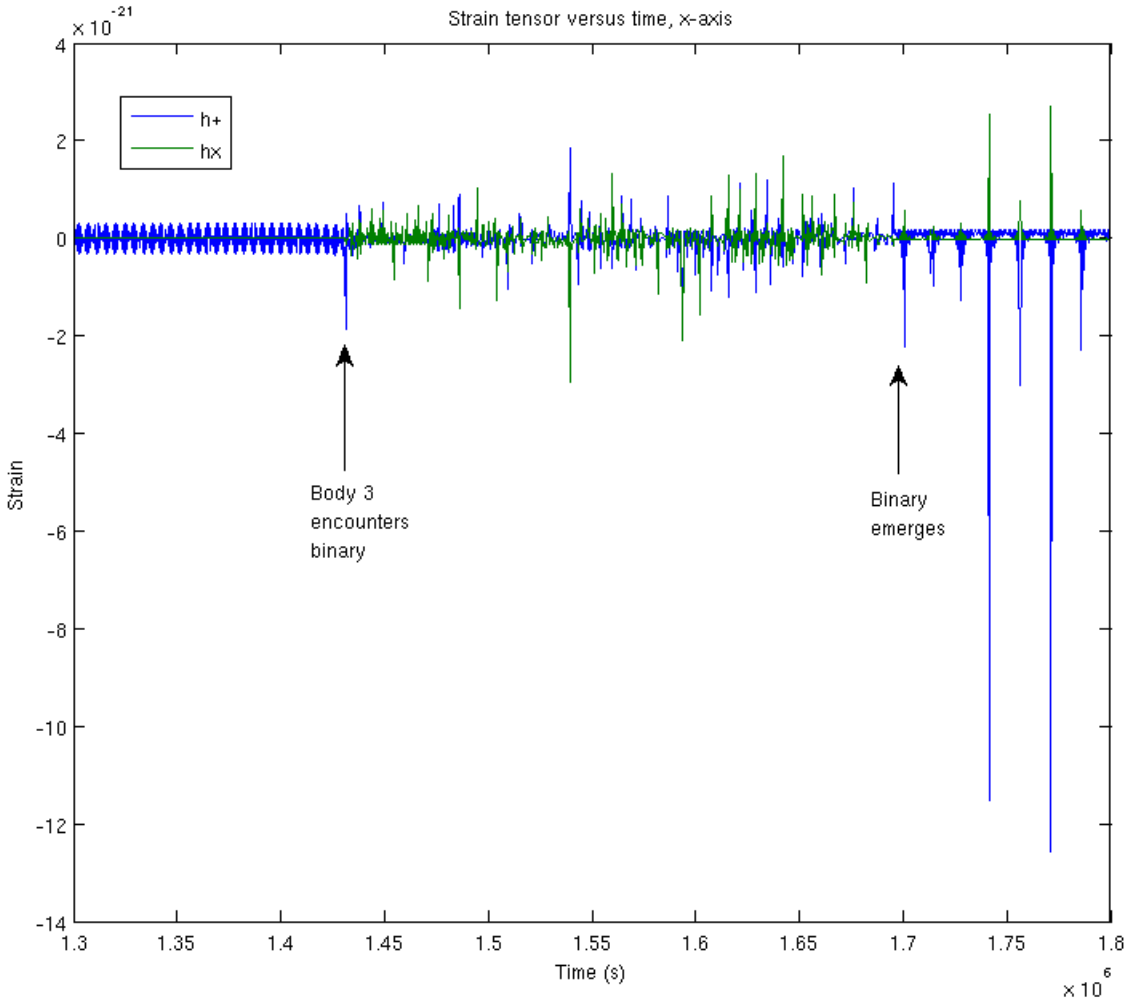

Figure 6: Strain tensor as a function of time in the x direction.

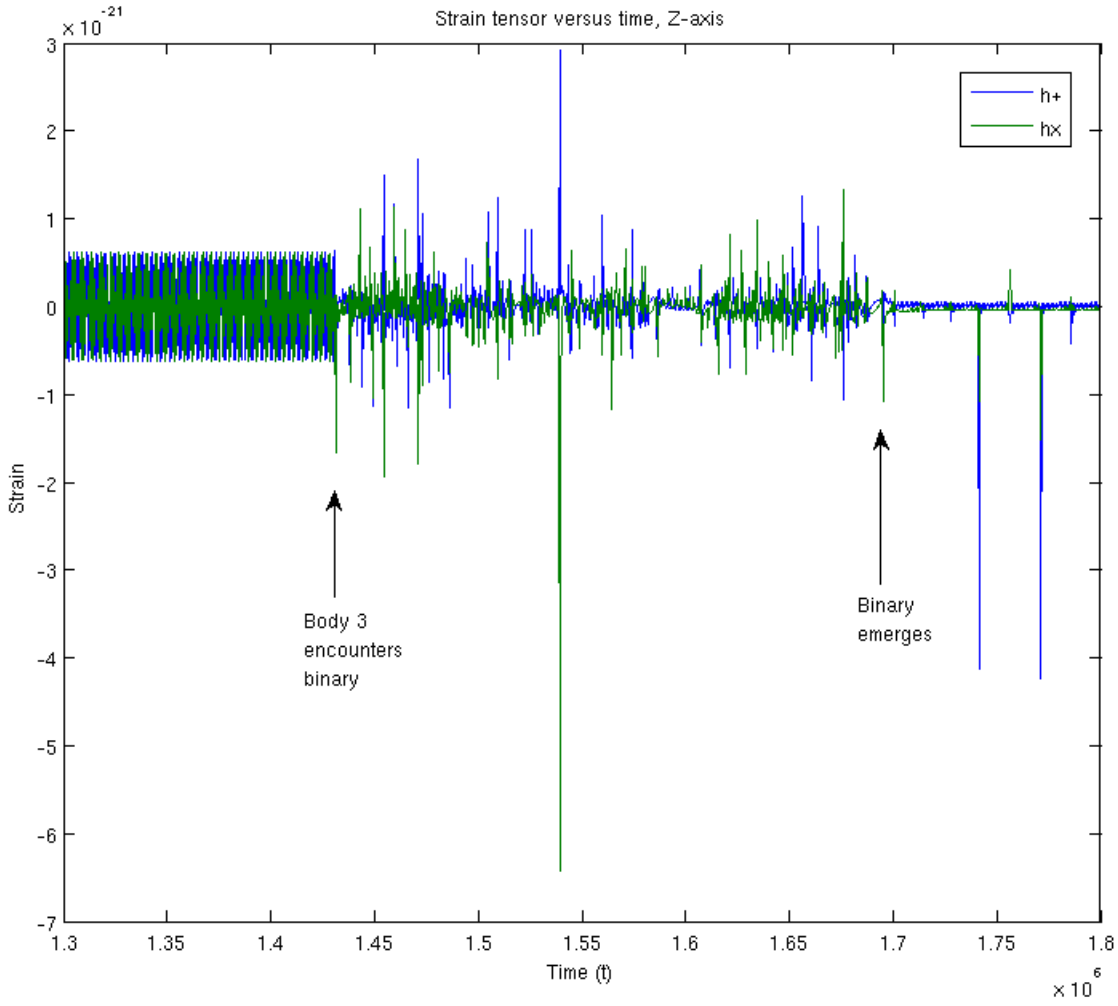

Figure 7: Strain tensor as a function of time in the z direction.

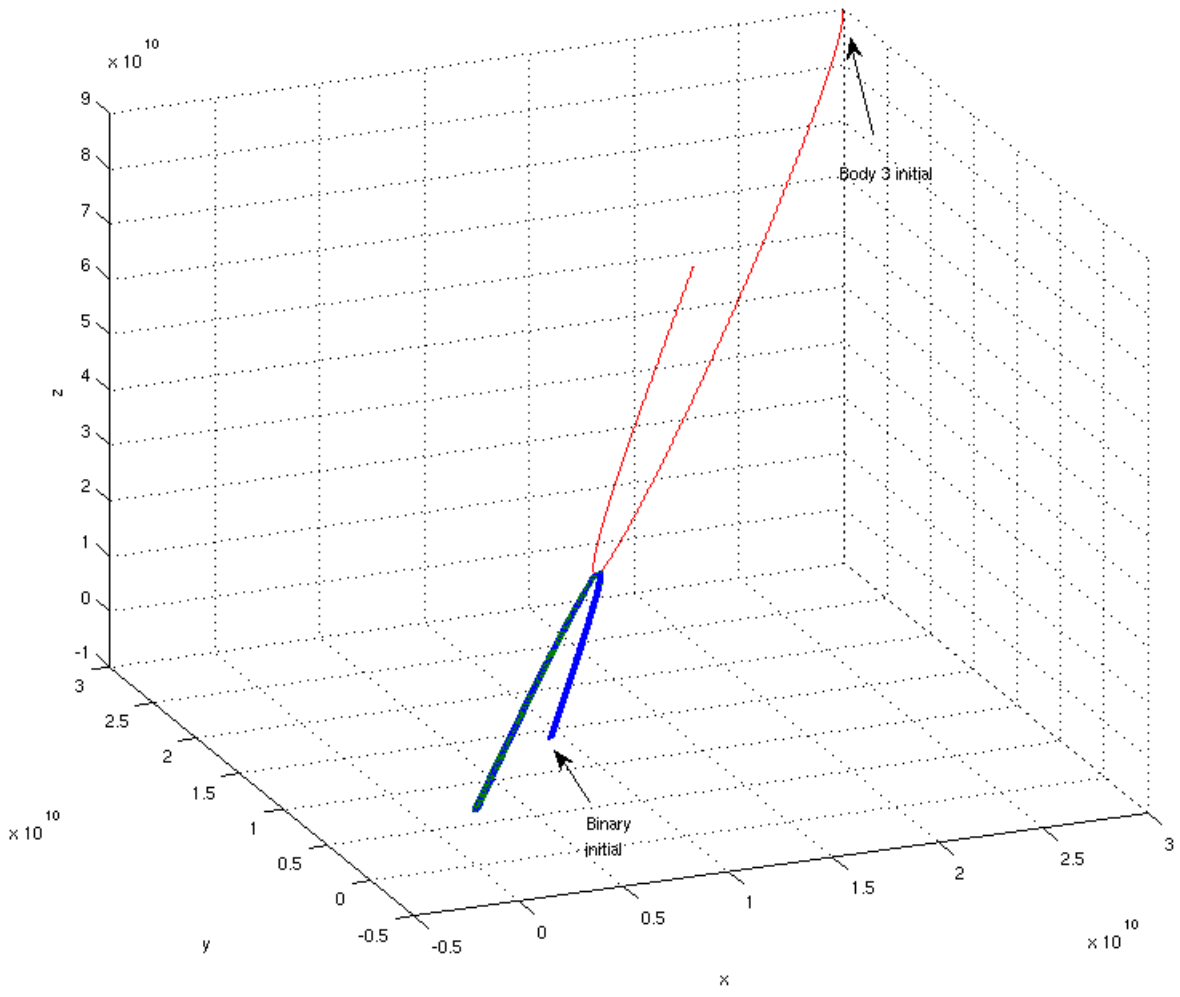

Figure 8: Trajectory of a "slingshot" interaction.

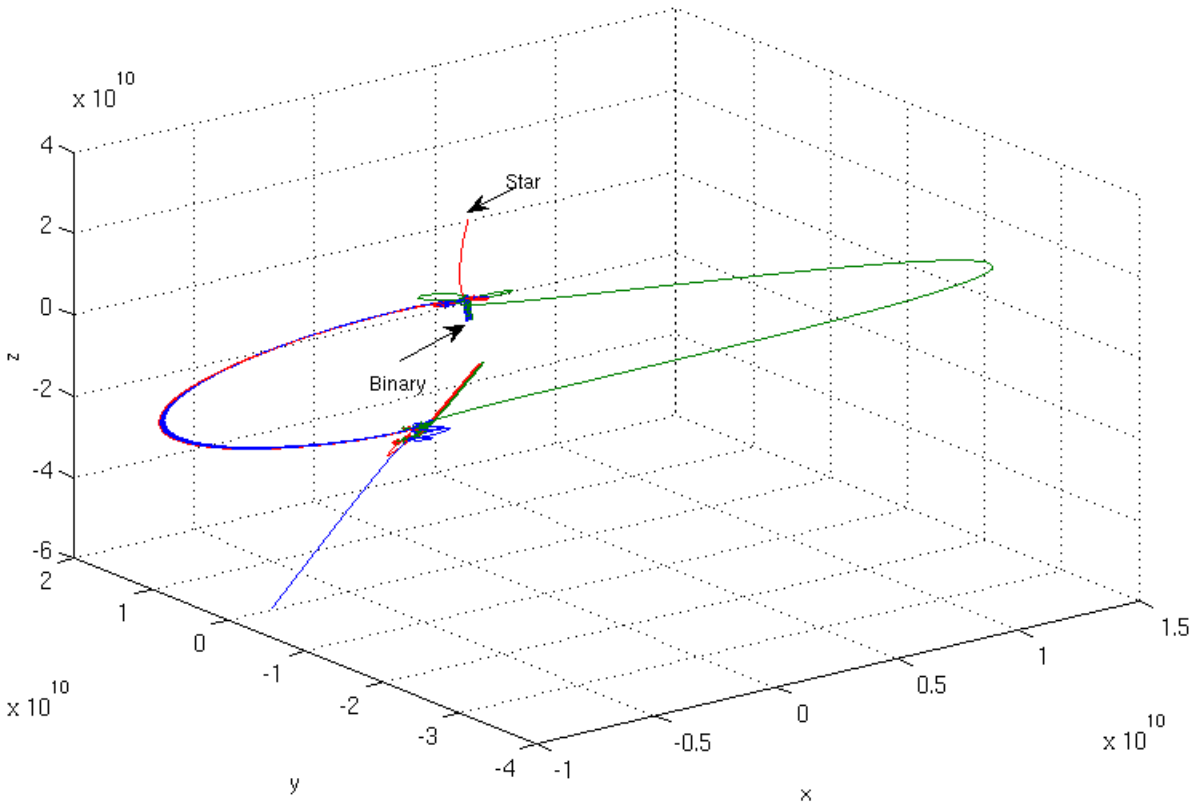

Figure 9: The trajectory for an interaction with 2 exchange/scattering events.

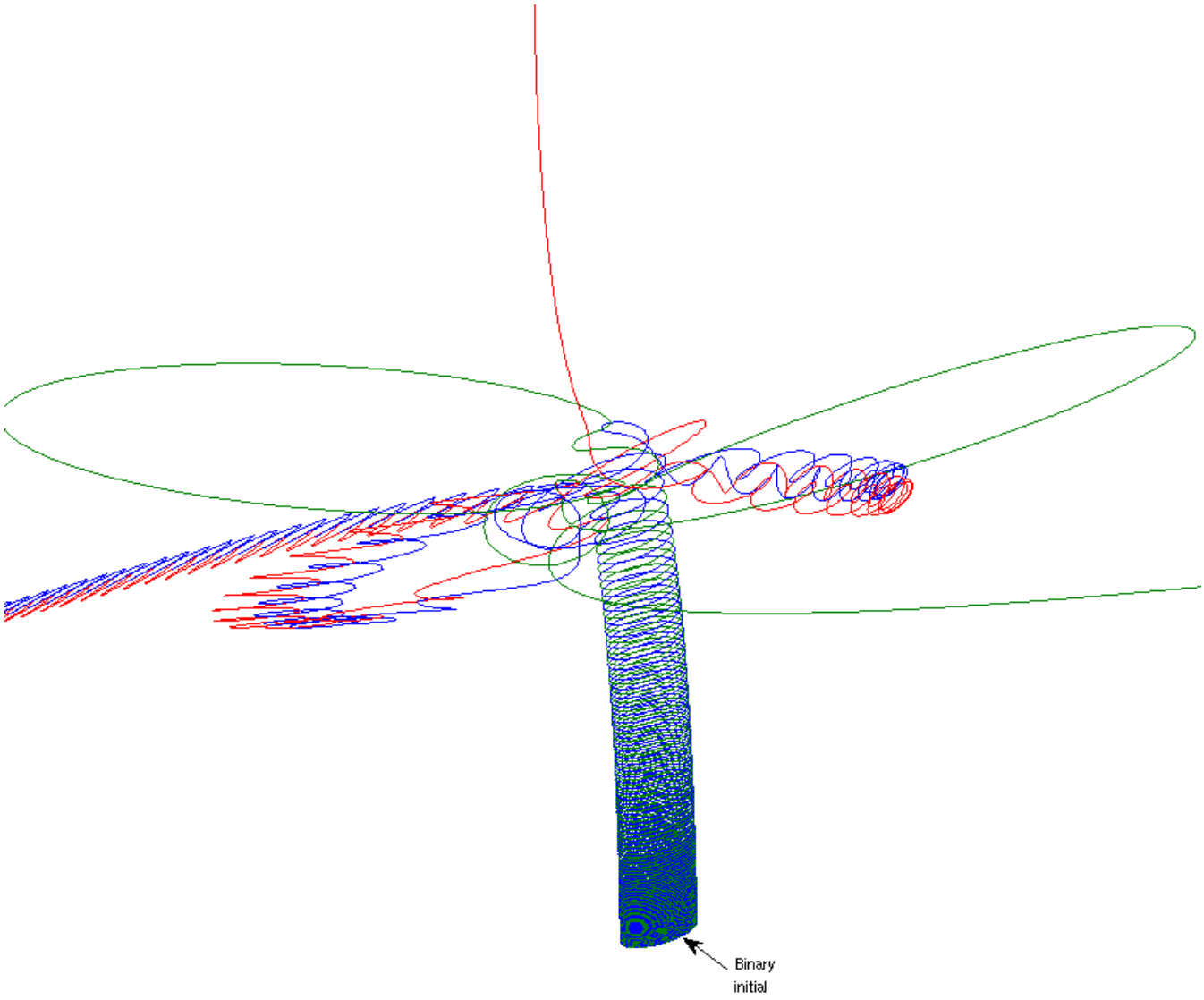

Figure 10: The first exchange interaction.

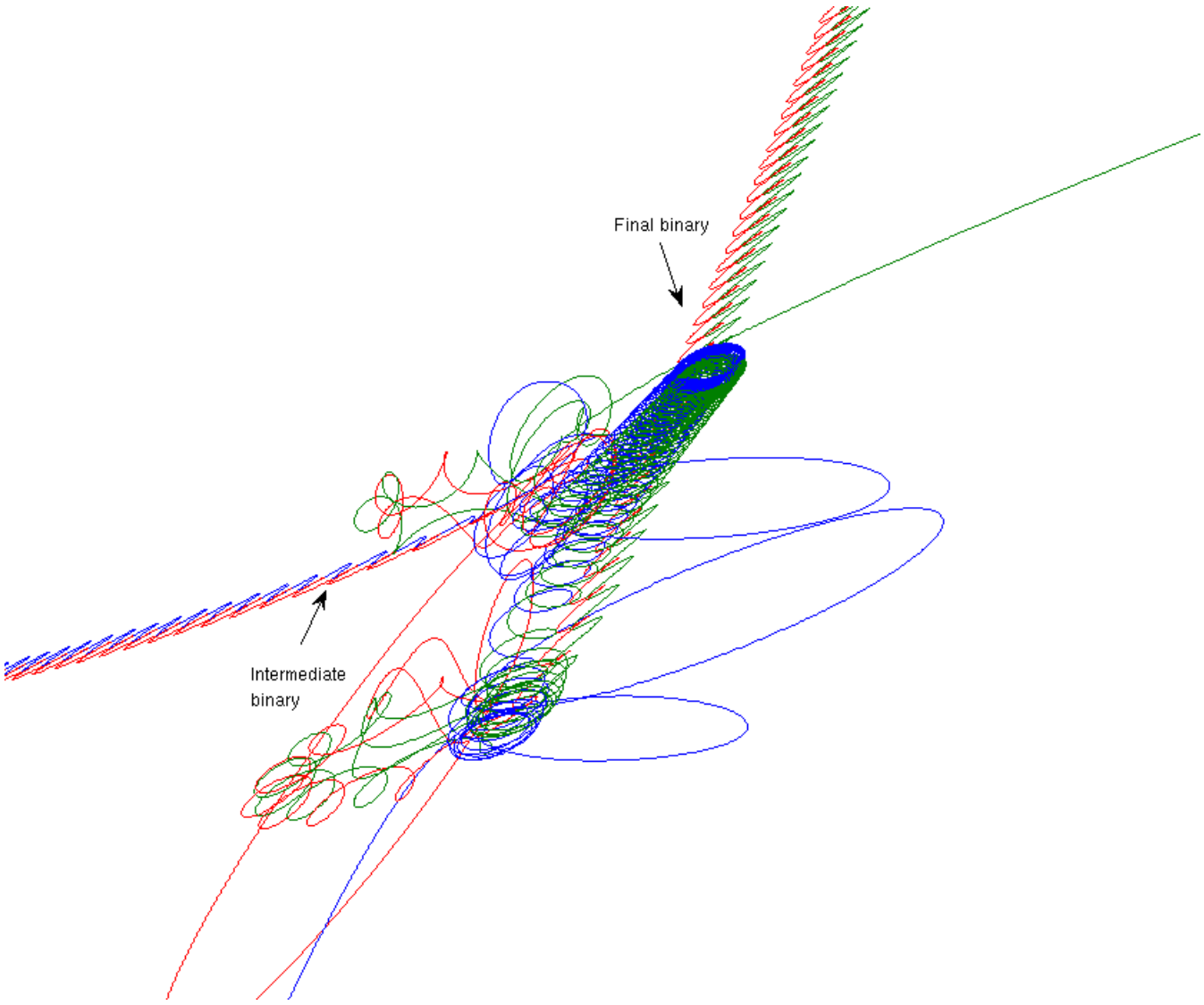

Figure 11: The second exchange interaction.

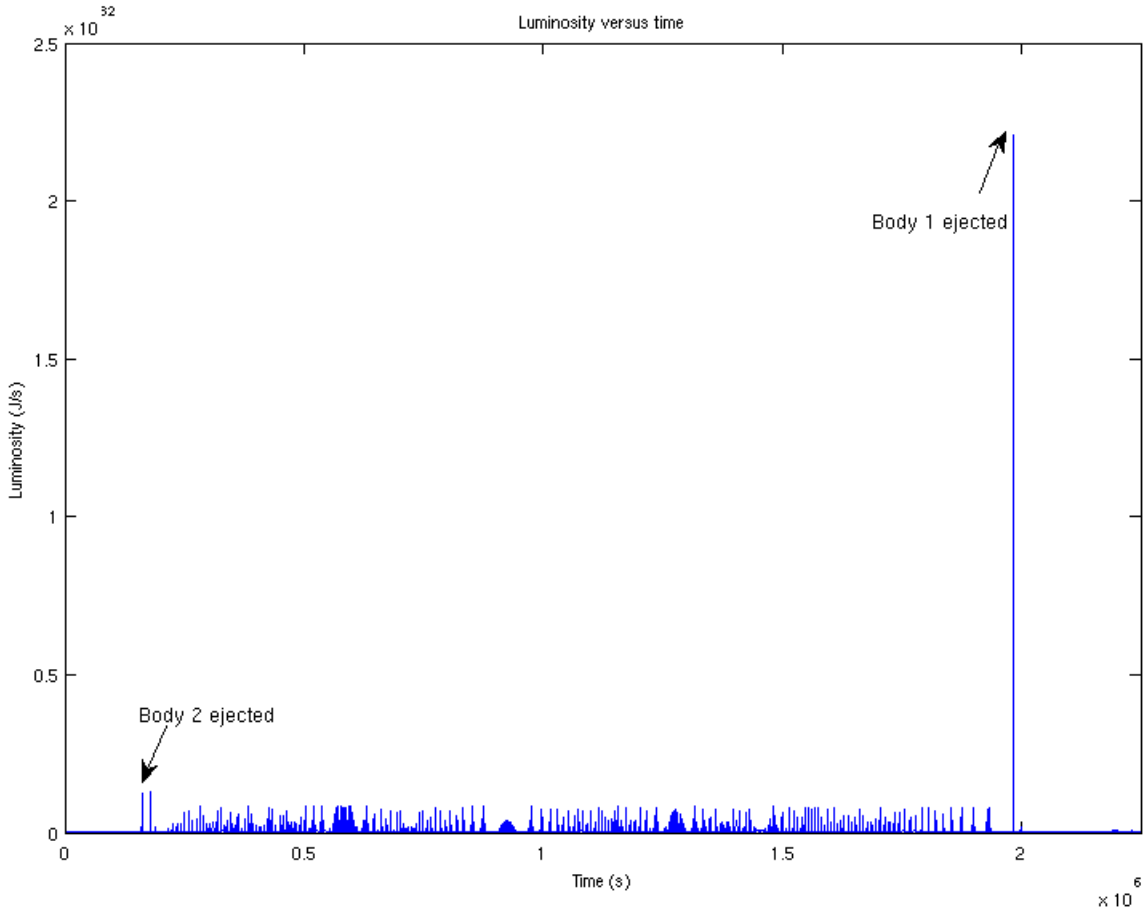

Figure 12: Luminosity versus time is shown.

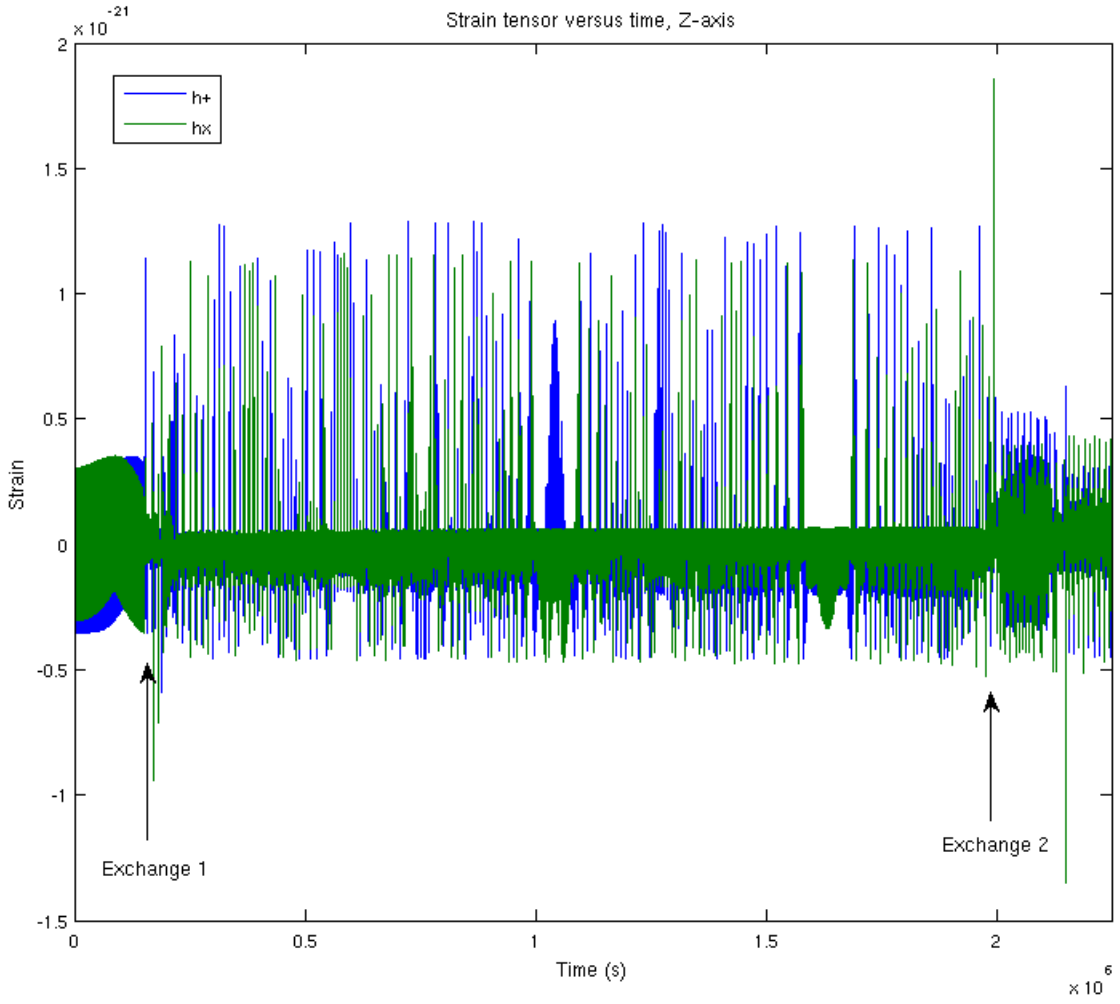

Figure 13: Strain tensor versus time for is shown. The solid color of the graph is due to the large time scale of the plot. The amplitudes are actually rapidly oscillating up and down; picture a sin curve being horizontally compressed into what looks like a rectangle. The same thing is happening here.

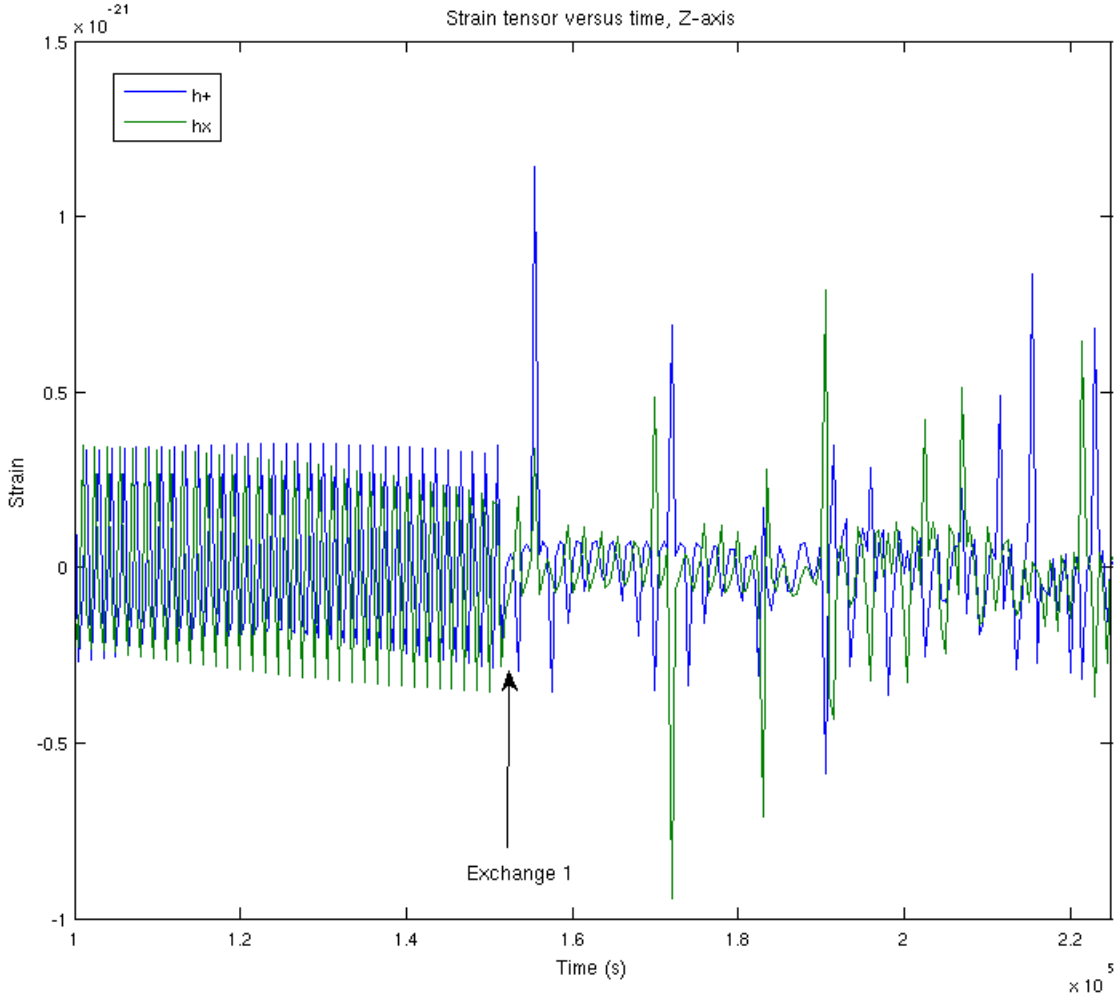

Figure 14: A closeup of the strain tensor plot versus time (see figure 13) during the first exchange event.

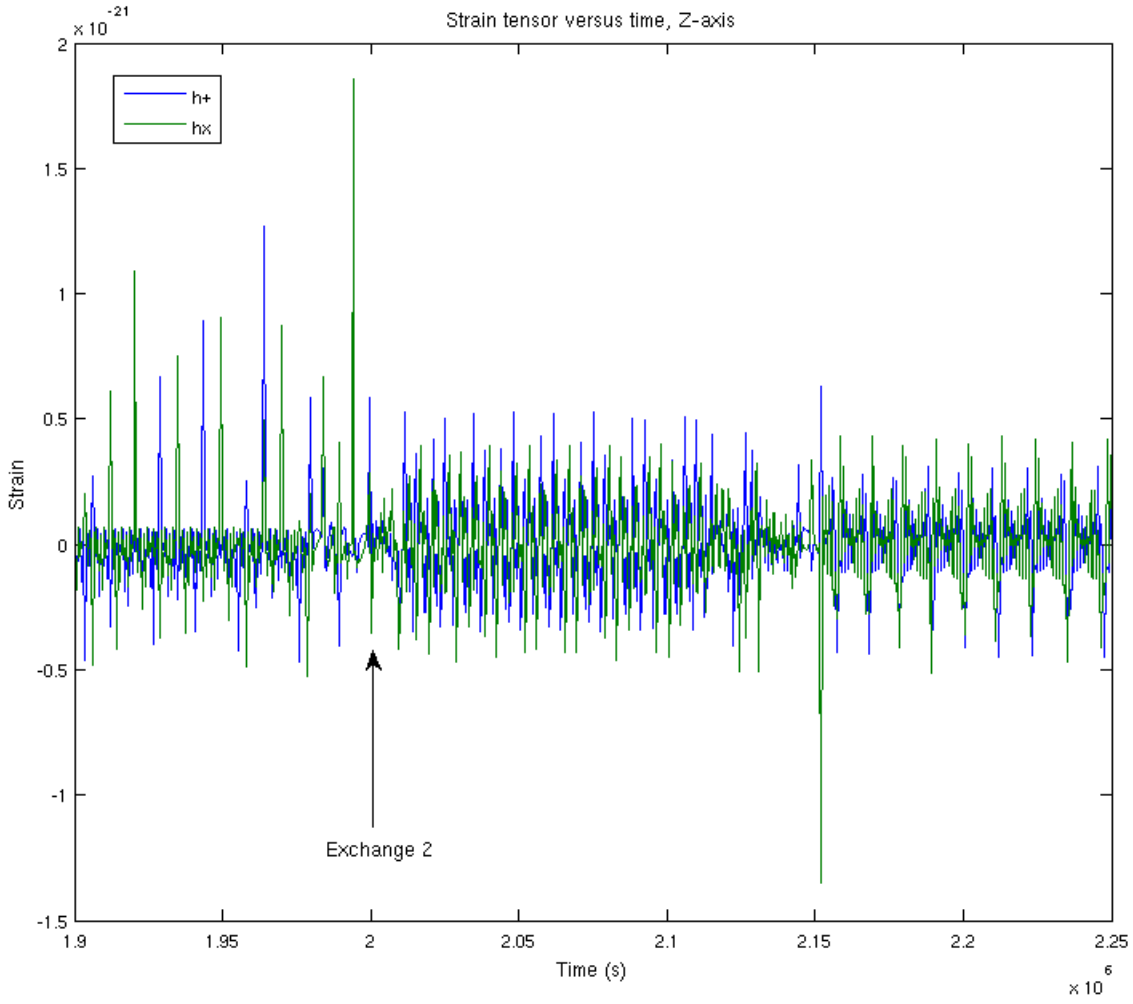

Figure 15: A closeup of the strain tensor plot versus time (see figure 13) during the second exchange event.

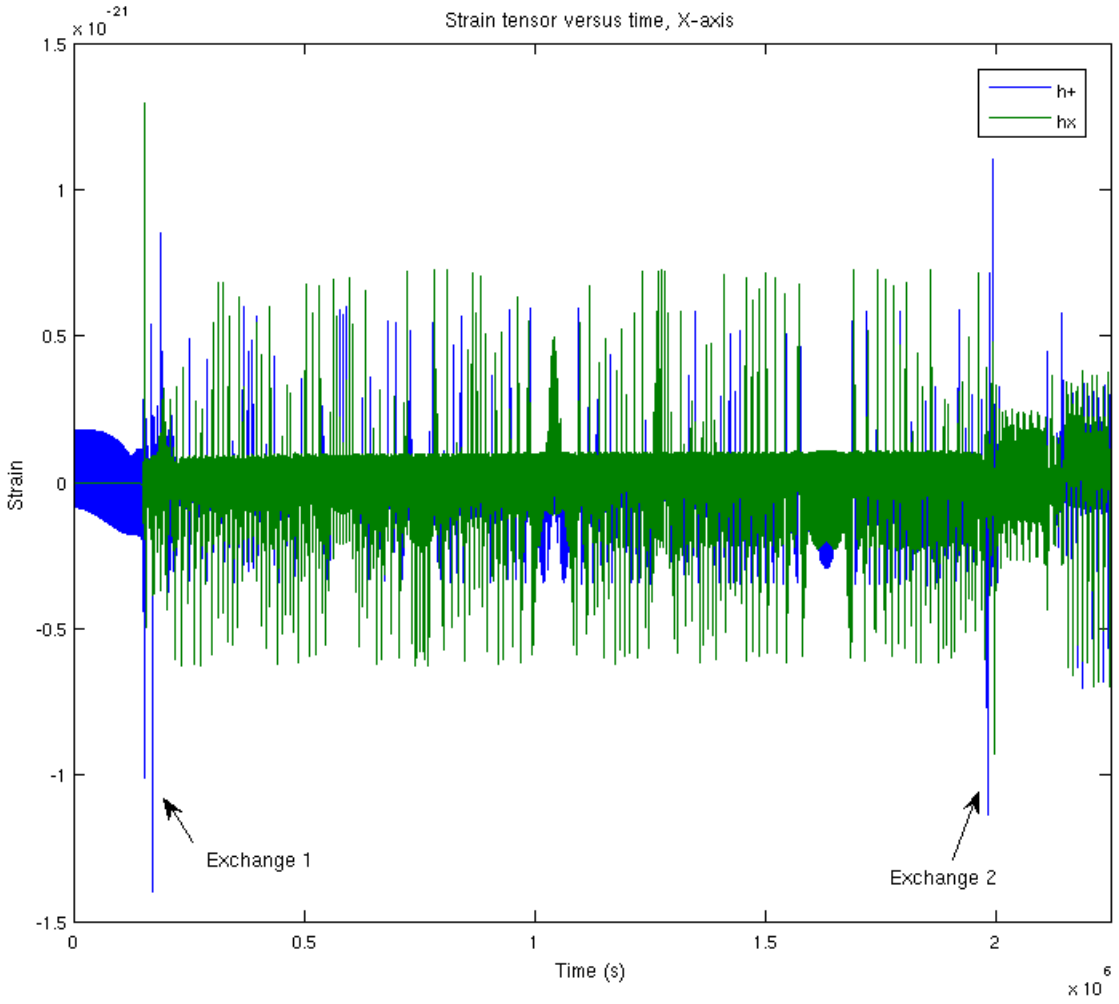

Figure 16: Strain tensor versus time in the x direction is shown.

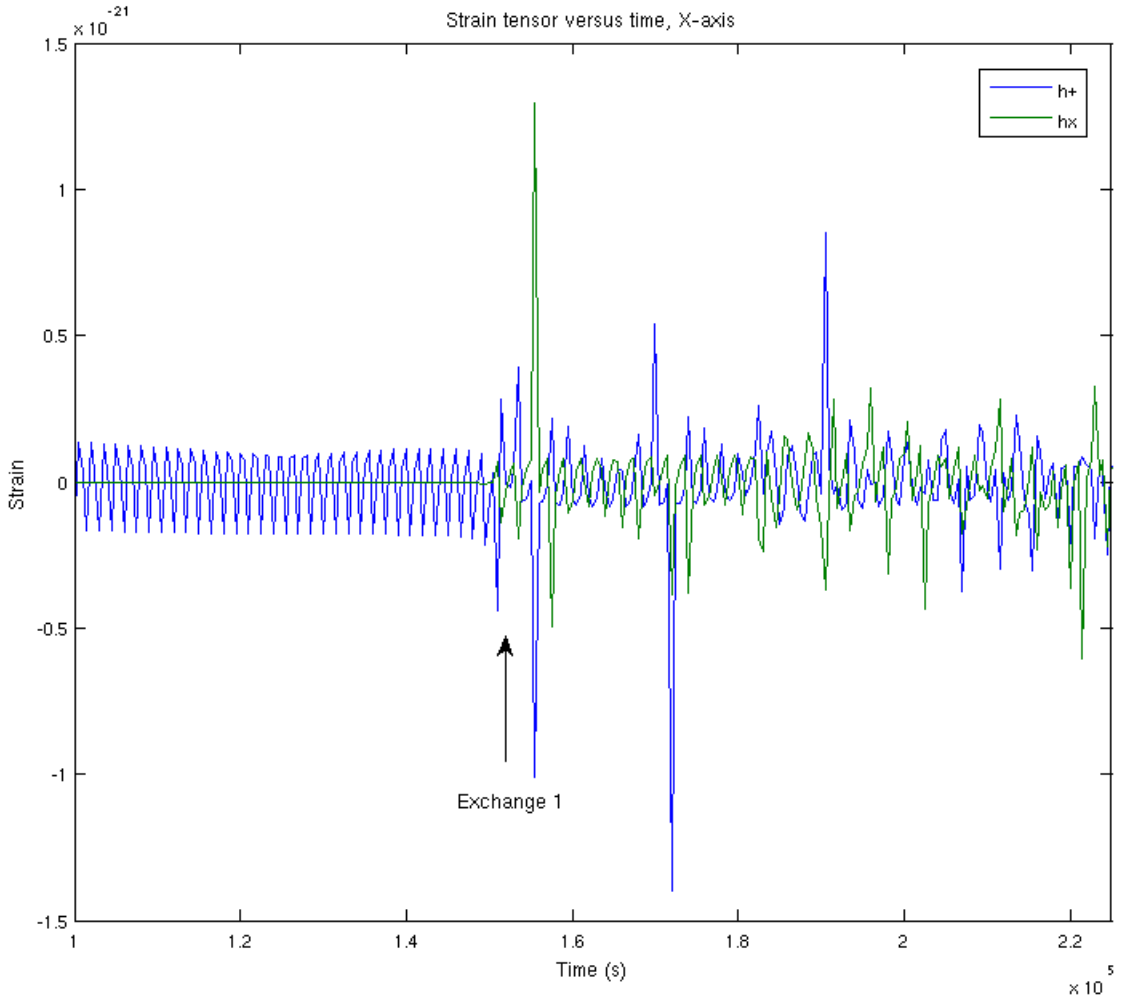

Figure 17: A closeup of the strain tensor plot versus time (see figure 16) during the first exchange event.

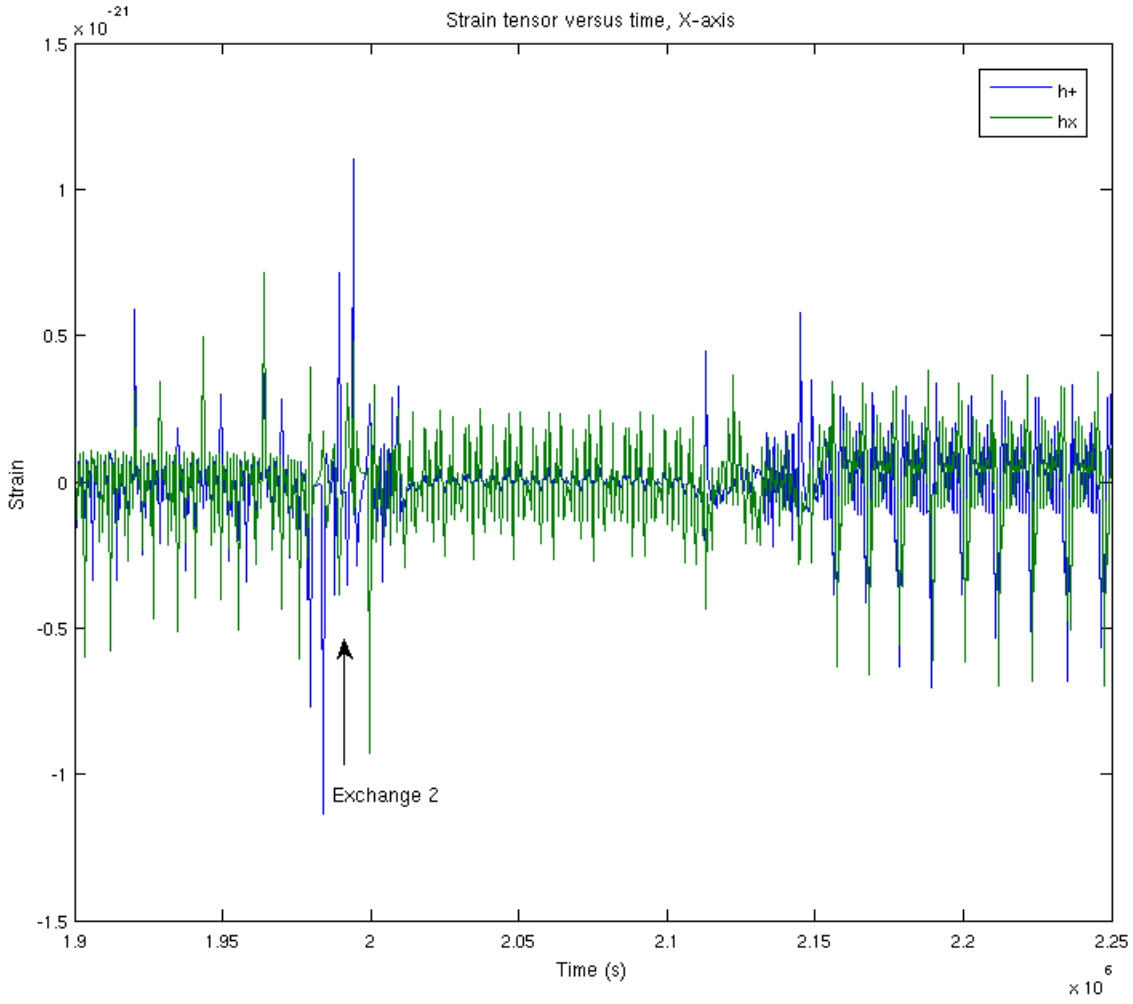

Figure 18: A closeup of the strain tensor plot versus time (see figure 16) during the second exchange event.

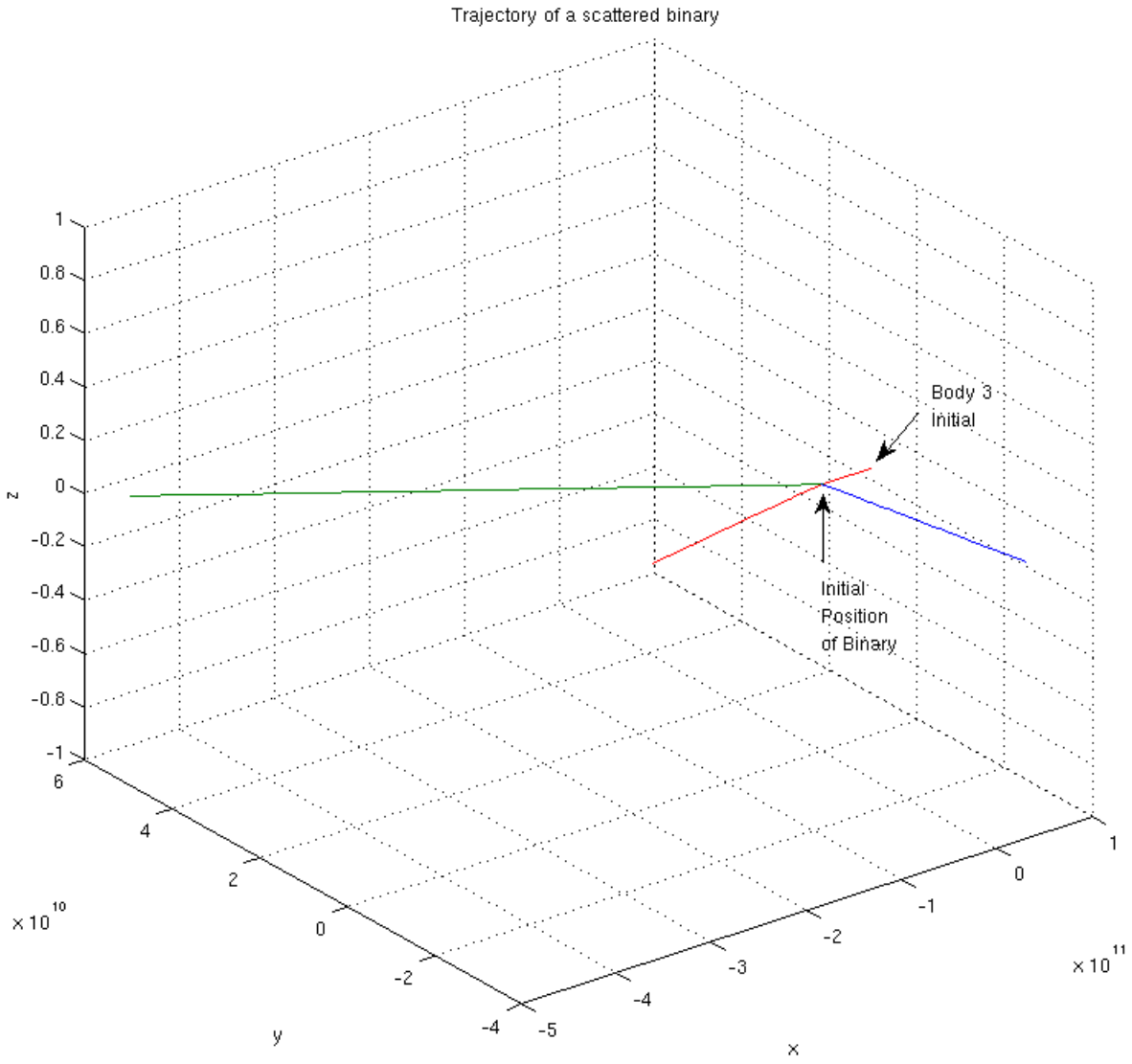

Figure 19: Body 3 passes near the binary with a high velocity, completely scattering bodies 1 and 2.

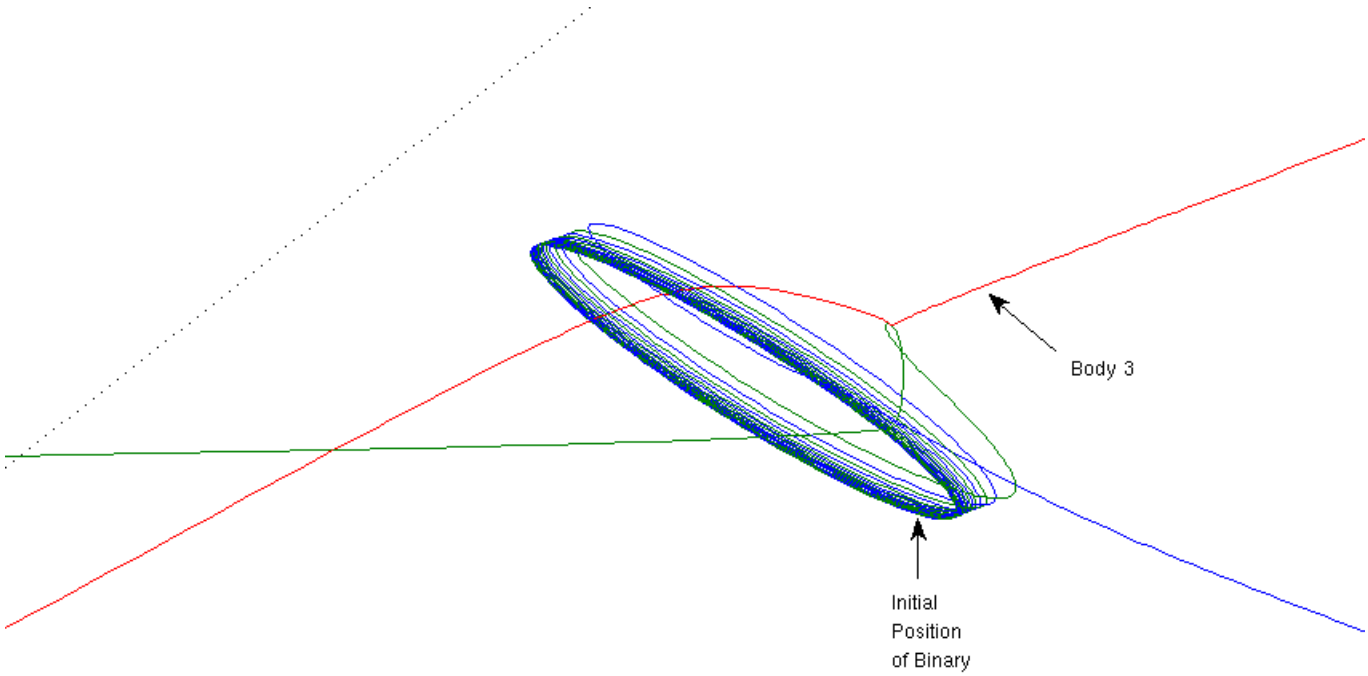

Figure 20: A close up of the scattering event.

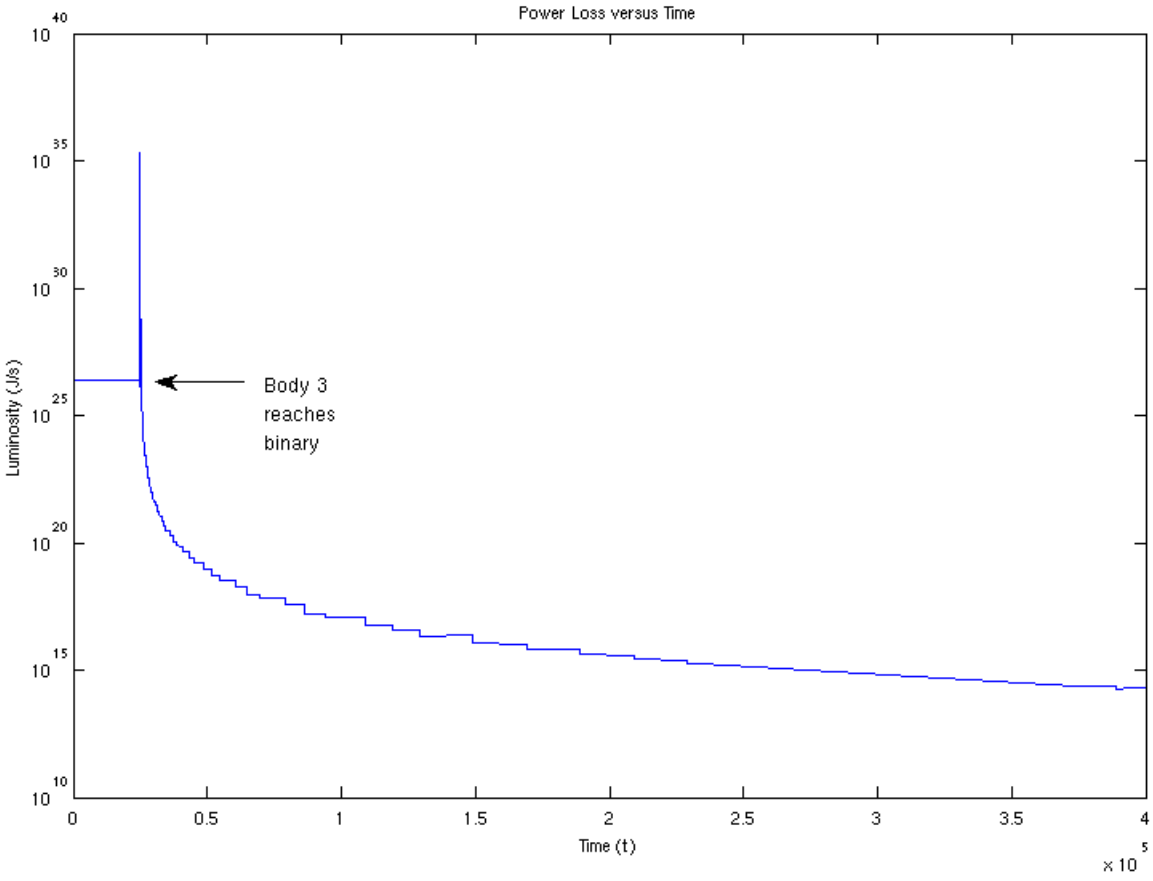

Figure 21: Luminosity as a function of time with a logarithmic scale.

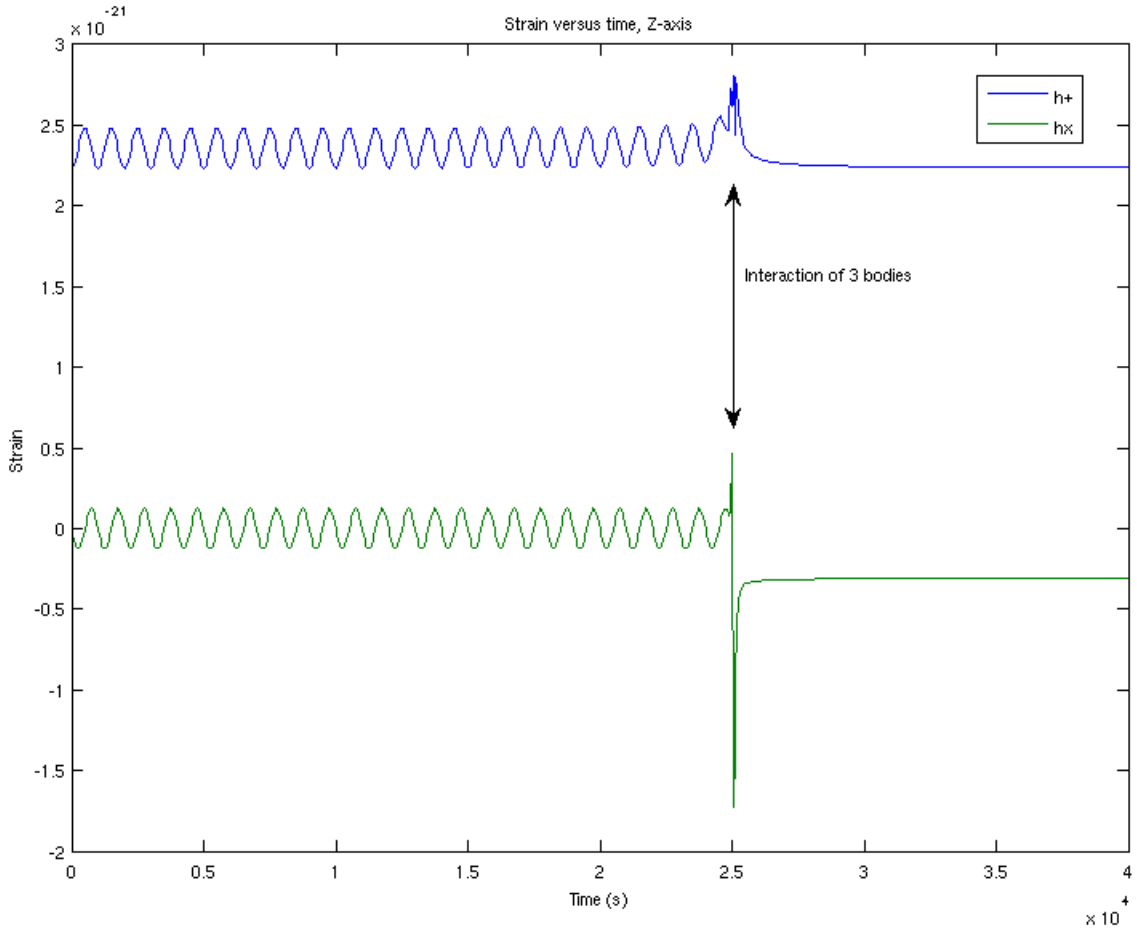

Figure 22: The components of the strain tensor as a function of time, as seen from the z-axis.

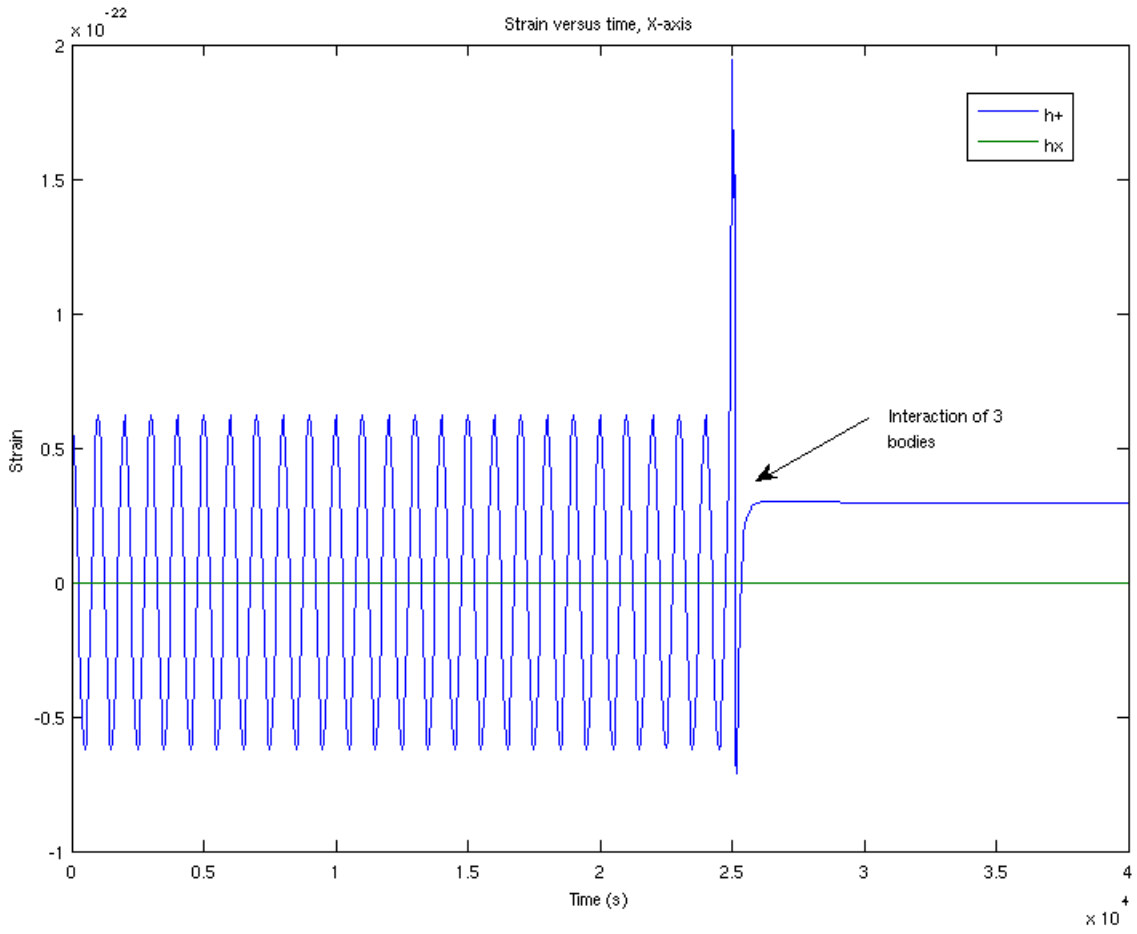

Figure 23: The components of the strain tensor as a function of time, as seen from the x-axis.

References

[1] J.H. Weisberg and J.H. Taylor. Relativistic Binary Pulsar B1913+16: Thirty Years of Observations and Analysis. ASP Conference Series (in press)

[2] NASA. Lisa Interferometer Space Antenna. Available at `http://lisa.nasa.gov/resources.html` (2008/07/20).

[3] J. Baker, P. Bender, P. Binetruy, J. Centrella, T. Creighton,J. Crowder, C. Cutler, K. Danzman, S. Drasco, L.S. Finn, C. Hogan, C. Miller, M. Milslavljevic, G. Nelemans, S. Phinney, T. Prince, B. Schumaker, B. Schutz, M. Vallisneri, M. Voloteri, and K. Willacy. *LISA: Probing the Universe with Gravitational Waves.* LISA Mission Science Office (19 Jan 2007).

[4] J. B. Hartle. *Gravity: An Introduction to Einstein's General Relativity.* Addison Wesley, San Francisco, CA (2003).

[5] L. Blanchet. Gravitational Radiation from Post-Newtonian Sources and Inspiralling Compact Binaries. Available at `http://relativity.livingreview.org/open?pubNo=lrr-2006-4` (2008/07/20)

[6] S. Sigurdsson and E.S. Phinney. Dynamics and Interactions of Binaries and Neutron Stars in Globular Clusters. Astrophysical Journal Supplements (in press)

A Index Notation and Summation Convention

In a 3-D coordinate system, standard notation is:

$$\vec{x} \equiv x, y, z \equiv x^i$$

where i runs from 1 to 3 and x^i denotes the i-th dimension. Thus, x^1 denotes x, x^2 denotes y, and x^3 denotes z. Spacetime coordinates use a similar system:

$$x^\mu \equiv t, x, y, z$$

where $0 \leq \mu \leq 3$ and x^0 denotes time.

Indices can either be above, as in x^μ or below, as in the strain tensor $T_{\alpha\beta}$; the two positions have different physical interpretations. For example, x^μ is a four-vector in spacetime whereas x_μ is called a dual vector and roughly represents planes orthogonal to x^μ. The two are related by:

$$x_\alpha \equiv \sum_{\alpha=0}^{3} g_{\alpha\beta} x^\beta$$

$$x^\alpha \equiv \sum_{\beta=0}^{3} g^{\alpha\beta} x_\alpha$$

where $g_{\alpha\beta}$ is the inverse of $g^{\alpha\beta}$.

In Einstein's summation convention, repeated indices indicate summations. The above equations can be rewritten as

$$x_\alpha = g_{\alpha\beta} x^\beta$$

$$x^\alpha = g^{\alpha\beta} x_\beta$$

So, in order to calculate I_{ij} from I^{ij},

$$I_{ij} = g_{i\alpha} g_{j\beta} I^{\alpha\beta}$$

Thanks to Phillip Zukin, whose notes provided a basis for this section.

B Integrator

Input was of the form $[x_1\ y_1\ z_1\ x_2\ y_2\ z_2\ x_3\ y_3\ z_3\ \dot{x}_1\ \dot{y}_1\ \dot{z}_1\ \dot{x}_2\ \dot{y}_2\ \dot{z}_2\ \dot{x}_3\ \dot{y}_3\ \dot{z}_3\ m_1\ m_2\ m_3]$

```
function dc = orbit33(t,c);
dc = zeros(21,1);
G = 6.673*10^(-11);
d12 = ((c(1)-c(4))^2+(c(2)-c(5))^2+(c(3)-c(6))^2)^.5;
d13 = ((c(1)-c(7))^2+(c(2)-c(8))^2+(c(3)-c(9))^2)^.5;
d23 = ((c(4)-c(7))^2+(c(5)-c(8))^2+(c(6)-c(9))^2)^.5;
m1 = c(19);
m2 = c(20);
m3 = c(21);
for i = 1:9
    dc(i) = c(i+9);
end
dc(10) = G*m2/(d12^3)*(c(4)-c(1))+G*m3/(d13^3)*(c(7)-c(1));
dc(11) = G*m2/(d12^3)*(c(5)-c(2))+G*m3/(d13^3)*(c(8)-c(2));
dc(12) = G*m2/(d12^3)*(c(6)-c(3))+G*m3/(d13^3)*(c(9)-c(3));
dc(13) = G*m1/(d12^3)*(c(1)-c(4))+G*m3/(d23^3)*(c(7)-c(4));
```

```
dc(14) = G*m1/(d12^3)*(c(2)-c(5))+G*m3/(d23^3)*(c(8)-c(5));

dc(15) = G*m1/(d12^3)*(c(3)-c(6))+G*m3/(d23^3)*(c(9)-c(6));

dc(16) = G*m1/(d13^3)*(c(1)-c(7))+G*m2/(d23^3)*(c(4)-c(7));

dc(17) = G*m1/(d13^3)*(c(2)-c(8))+G*m2/(d23^3)*(c(5)-c(8));

dc(18) = G*m1/(d13^3)*(c(3)-c(9))+G*m2/(d23^3)*(c(6)-c(9));

dc(19) = 0;

dc(20) = 0;

dc(21) = 0;
```